

MARCH 1978

INT 89/78

DEVELOPMENT OF AN ION BEAM PROBE DIAGNOSTIC SYSTEM

Part I

Principle and Description of the Project

G. Tonetti

Centre de Recherches en Physique des Plasmas

ECOLE POLYTECHNIQUE FEDERALE DE LAUSANNE

## I INTRODUCTION

One of the main problem about studying thermonuclear plasma devices is the lack of diagnostic methods to measure the electromagnetic field inside the plasma. Methods using laser or microwaves have been proposed, but few of them are yet feasible.

The aim of this report is to propose the development of an ion beam probe diagnostic system (IBP) that should allow such measurements.

The IBP is a not well known diagnostic method that has been developed during the last few years<sup>1-4</sup>. It is nonperturbing for the plasma and it has both space and time resolutions. Its present capabilities include the measurement of the electron density, the electron temperature, and the electric potential.

Theoretical calculations and computer simulations have shown that the magnetic potential should also be directly and locally measurable in an axisymmetric device such as a tokamak<sup>5</sup>. This would be a very interesting measurement since it is directly related to the structure of the magnetic surfaces, the poloidal field and the current density in the plasma. The experimental demonstration of this measurement is, however, still to be done.

## II PRINCIPLE OF THE ION BEAM PROBE

The basic principle is illustrated in Fig. 1. A beam of monoenergetic singly charged primary ions (the primary beam) is directed through the system normal to the main confining magnetic field. During the transit through the plasma, some of these primary ions will undergo collisions with the plasma particles, the most probable process being secondary

ionizations by collision with the plasma electrons. The main feature of the IBP is that this type of collision does not change appreciably the momentum of the ions (their mass being much larger than the electron one). Thus, test particles with known initial conditions are created inside of the plasma. These test particles, or secondary ions, are separated from the primary beam by the magnetic field and go out of the plasma. The entrance slit of an appropriated detector intercepts a part of these secondary ions (the secondary beam) coming from a small volume of plasma centered around the corresponding secondary emission point.

By sweeping and changing the energy of the primary beam (Fig. 2), any points in a given volume of plasma can be observed by the detector with both space and time resolutions. Furthermore, the density of ions in the beam being much smaller than the plasma density, the measurement is non perturbing.

The local information at the secondary emission point carried out by the ions is of two kinds. The current of ions is related to the electron density and temperature and their energy and momentum are related to the electromagnetic potentials.

### III IONIZATION PROCESSUS AND MEASUREMENTS OF THE ELECTRON DENSITY AND TEMPERATURE

The current of secondary ions created inside of the plasma is given by :

$$I^{++} = I^+ \cdot n_e \cdot \ell \cdot \frac{\langle \sigma \cdot v_r \rangle}{v_i} = I^+ \cdot n_e \cdot \ell \cdot \tilde{\sigma} \quad (1)$$

where  $I^+$  is the local current of primary ions  
 $n_e$  is the electronic density  
 $l$  is the length of primary beam  
 $\sigma$  is the cross section for  $A^+ + e^- \rightarrow A^{++} + 2e^-$   
 $v_r$  is the relative electron - ion speed  
 $v_I$  is the ion speed

Other kinds of collisions can also produce secondary ions. But, the effective cross section  $\hat{\sigma}$  for collision with the electrons is enhanced by a factor of about 100 over the other processes due to the averaging  $\langle \sigma \cdot v_r \rangle$ . Furthermore, most of the other processes, such as collision with the plasma ions, will change the momentum of the probing ions. An energy selective detector should then be able to separate these sources of noise from the interesting signal.

For density  $n_e$  of  $10^{13}$  p/cm<sup>3</sup> and a primary ion beam of 1  $\mu$ Amp, the ratio  $I^{++}/I^+$  is typically of the order of 0.01 - 0.1 per centimeter of beam length. The current of secondary ions at the detector will then be of the order of few nAmps which should be easily measurable with a carefully designed detector system.

Note that for temperatures higher than 100 eV, the density is limited to about  $10^{14}$  p/cm<sup>3</sup>. At higher densities, the ion beam quickly attenuates in the plasma.

### 1. Measurement of the Electron Density and Temperature

The current of secondary ions measured outside of the plasma contains information about the electronic density and temperature (through  $\hat{\sigma}$ ). But it also depends upon the geometrical factor  $l$  and the attenuation of the beams across the plasma. The geometrical factor can easily be determined

by the calculation of the ions trajectories, whereas the effects of the attenuation can be taken into account by an iteration.

To measure the electron temperature, one uses two types of ions with different cross sections. The energies are scaled to reproduce the same trajectories for both types of ions. By taking the ratio of the currents, the dependence upon the density and the geometrical factor cancels. If, for the moment, one neglects the attenuation of the beams, one obtains :

$$\frac{(I^{++}/I^+)_{A}}{(I^{++}/I^+)_{B}} = \frac{n_e \cdot \ell \cdot \hat{\sigma}_A(T_e)}{n_e \cdot \ell \cdot \hat{\sigma}_B(T_e)} = f(T_e) \quad (2)$$

Fig. 3 shows a typical effective cross section  $\hat{\sigma}$  and the function  $f(T_e)$  for sodium and potassium ions. The averages have been calculated with a Maxwellian distribution for the electron speed. With other types of ions, different ranges of temperature up to few 100 eV are measurable.

Once the temperature has been determined, the density can be computed from the ratio  $I^{++}/I^+$  for either ions. However, for temperatures lower than 100 eV, a small error on the temperature measurement can introduce a large error on the density. This is due to a sharp decrease of  $\hat{\sigma}(T_e)$  (Fig. 3) below 100 eV.

It is then clear that the IBP cannot make both measurements accurately in every condition. For a low temperature plasma ( $< \sim 100$  eV), the temperature can be easily measured, but the density is entatched of a large error. At high temperature ( $> \sim 1$  KeV) it is not possible to find a pair of ions for which  $f(T_e)$  is usable. The density, however, can be accurately determined if the temperature is known by any other measurements.

Despite these difficulties, the IBP may still be very interesting to use because of its large recording capacity given by the possibility of sweeping the beam .

## 2. Density Fluctuations

In a high temperature plasma ( $\geq 100$  eV), the weak dependence of  $\hat{\sigma}$  upon the temperature requires that the fluctuations of  $I^{++}$  are caused mainly by density fluctuations. The modulation of the current includes the local effect of the fluctuations at the secondary emission point and the total effect of the fluctuation along the trajectories. If the fluctuations are relatively localized, only the first effect will be important and the measurement of  $I^{++}/I^{++}$  will be a direct measurement of the local density fluctuation. It is not yet clear what can be the resolution of such a measurement and its limitation in frequency.

## IV DYNAMICS OF THE IONS AND MEASUREMENT OF THE ELECTROMAGNETIC POTENTIALS

The easiest way to investigate the dynamics of the probing ions in the system of Fig. 1 is to use the symmetries and the related conservation laws. The possibility of measuring the electric potential follows from the energy conservation. If the system is time invariant, or more exactly, if during the transit of the ions through the system (the measurement time) the fields do not change very much, the total energy of the ions

$$W = T + qV \quad (3)$$

where  $T$  is the kinetic energy  
 $V$  is the electric potential  
 $q$  is the charge

is a constant of the motion. The secondary ionization by collision with the plasma electrons does not change appreciably the kinetic energy of the ions. Therefore, one has for the total energy on the primary ( $\Gamma_1$ )

and secondary ( $\Gamma_2$ ) trajectories (see Fig. 1)

$$\begin{aligned}\Gamma_1) \quad T_G + qV_G &= T_I + qV_I \\ \Gamma_2) \quad T_D + 2qV_D &= T_I + 2qV_I\end{aligned}\tag{4}$$

The plasma potential at the secondary emission point,  $V_I$ , can then be related to the external kinetic energies by taking the difference between these two equations. This gives :

$$V_I = \frac{1}{q} (T_D - T_G)$$

where the constant term  $2V_D - V_G$  has been dropped out, the potential being defined to a constant.

The energy of the primary ions is known, therefore, by measuring the energy of the secondary ions,  $T_D$ , at a fixed point outside of the plasma, one has a direct determination of the electric potential at the secondary emission point.

Components of the magnetic vector potential can also be measured if the plasma system is axisymmetric. Then, the fields are not a function of the corresponding ignorable coordinates  $x_i$  and the conjugated components of the canonical momentum

$$P_i = p_i + qh_i A_i\tag{5}$$

where  $\vec{p}$  is the kinetic momentum

$\vec{A}$  the vector potential

$h_i$  the metric coefficient of the coordinate system used to describe the system

$q$  the charge of the ions

are constants of the motion.

As before, because the ion momentum is not changed by the secondary ionization, one can write the following relations on the trajectories :

$$\begin{aligned} \Gamma_1) \quad p_{iG} + q(hiAi)_G &= p_{iI} + q(hiAi)_I \\ \Gamma_2) \quad p_{iD} + 2q(hiAi)_D &= p_{iI} + 2q(hiAi)_I \end{aligned} \quad (6)$$

The quantity  $hiAi$  at the secondary emission point can be directly related to the external momentums by taking the difference between these equations. After dropping a constant term, one gets

$$(hiAi)_I = \frac{1}{q} (p_{iD} - p_{iG}) \quad (7)$$

The initial momentum  $\vec{p}_G$  is known, thus by determining the component of the velocity of the secondary ions in the direction of invariance of the system one has a direct measurement of the corresponding component of the vector potential at the secondary emission point. The other components that are not related to an ignorable coordinate cannot be directly measured in this way. The external momentum depends then upon the fields all along the trajectories of the ions.

#### 1. Position of the secondary emission points

It is important to note that the previous calculations gave us the value of the potentials at the secondary emission points, but no information about the location of these points, which are of course determined by the fields. In consequence, it is necessary that the trajectories of the



probing ions are only weakly dependent on the unknown part of the fields to be measured. The secondary emission points can then be approximated by computing the trajectories in the known part of the field only. Hopefully in most of the plasma devices these conditions are fulfilled. The main confining field is generally known and the perturbations created by the plasma are small. Furthermore, a self consistent iteration scheme can easily be applied to obtain both the unknown fields and the exact location of the secondary emission points. The convergence of such an iteration has been demonstrated by computer simulations<sup>5</sup>.

#### V APPLICATION TO A TOKAMAK

Tokamaks are very well suited for ion beam probing. The plasma densities and temperatures allow the penetration of the beam through the system and the symmetries are such that one should be able to measure the electric potential and the toroidal component of the magnetic potential. Furthermore, the relative magnitude of the fields is such that the position of the secondary emission points can be computed with the known toroidal field only.

The range of energies necessary to look at a given volume of plasma depends upon the magnitude of the toroidal field and on the relative gun detector position. To keep the energy at a reasonable value, one uses heavy ions such as cesium or thallium.

The transit time of the ions from the gun to the detector is of the order of few  $\mu$ s which is much shorter than the characteristic time variation of the tokamak fields ( $\sim$  ms). The time invariance can then be supposed to be satisfied which means that the electric potential should be measurable.

Ideal tokamaks are axisymmetric devices. Then, the toroidal component of the magnetic vector potential should be measurable by determining the velocity of the secondary ions in the toroidal direction. But, because of the spacing between the coils, the toroidal field is always slightly corrugated which destroys the symmetry. Therefore, to be able to carry out this measurement, it is necessary that the effects of this corrugation on the trajectories of the ions are small in comparison to the deflection caused by the poloidal field. These conditions can be satisfied if the trajectories stay close to the midplane between the coils where the effects of the corrugation are minimum.

The measurement of the toroidal component of the velocity,  $V_T$ , of the secondary ions gives the value of  $h_T A_T$  at the secondary emission point. The position of the magnetic surfaces in the plasma are directly related to this measurement by the relation

$$(h_T A_T)(\vec{r}) = \text{constant} \quad (8)$$

The two components of the poloidal field are then given by :

$$\begin{aligned} B_r &= \frac{1}{h_r h_\theta} \cdot \frac{\partial (h_T A_T)}{\partial \theta} \\ B_\theta &= \frac{-1}{h_r h_r} \cdot \frac{\partial (h_T A_T)}{\partial r} \end{aligned} \quad (9)$$

and the toroidal current density follows as

$$\mu_0 \dot{j}_T = \frac{1}{h_r h_\theta} \left( \frac{\partial (h_\theta B_\theta)}{\partial r} - \frac{\partial (h_r B_r)}{\partial \theta} \right) \quad (10)$$

Two other pieces of information are given by this measurement. First, the magnetic axis is at the point where the quantity  $h_T A_T$  is maximum, i.e. it is located at the secondary emission point where the secondary ions show a maximum  $v_T$  velocity.

The second piece of information is given by measuring the potential as a function of the time. The emf field that drives the toroidal plasma current is then given by

$$E_T = - \frac{\partial(h_T A_T)}{\partial t} \quad (11)$$

This field and the current density (10) give the plasma resistivity

$$j_T = \sigma E_T \quad (12)$$

To obtain the poloidal field and the current density, derivatives of the measured potentials have to be taken. To lose a minimum of accuracy through these calculations, one has to be careful about the numerical manipulations of the data.

Plasma temperatures in tokamaks are too high to be measured with the IBP. However, density profiles and density fluctuations are easily measurable, the effective cross section  $\hat{\sigma}$  being weakly dependent of the temperature.

## VI CONSTITUTIVE PARTS OF AN IBP

An IBP diagnostic system is made up of 6 parts :

1. The ion gun
2. The detector
3. The accelerating voltage supplies
4. The electronic system for the detector
5. A data acquisition system
6. The software to reduce the data

The two first parts will be discussed in this report, the rest being usual.

### 1. The Ion Gun

For energies lower than 100 keV, simple ion guns can be made as shown in Fig. 4. The gun includes an ion emitter, the focusing and accelerating electrodes, the deflecting plates.

#### 1.1 The Ion Source

The ion emitter (Fig. 5) is made of a ceramic support filled with zeolite and heated by a tungsten filament. The zeolite<sup>6</sup> is an artificial aluminosilicate crystal that can be loaded with alkalin ions ( $\text{Li}^+$ ,  $\text{Na}^+$ ,  $\text{K}^+$ ,  $\text{Rb}^+$ ,  $\text{Cs}^+$ ). These ions are extracted from the crystal by heating it at about  $1000^{\circ}\text{C}$  and applying an electric field to the surface. Ion sources of 100  $\mu\text{Amps}$  can easily be obtained with a life duration of 100 to 300 hours. No neutral emissions from these sources have been observed which makes them very suitable for high vacuum operation. Furthermore, contact with the atmosphere does not affect their properties.

The ion source is completed by an extractor called a Pierce gun<sup>7</sup>. The extractor surfaces are shaped (Fig. 6) to produce a field between the electrodes that both accelerate the ions and balance the radial forces of the space charges in the beam. The ion current is controlled by the extractor voltage as  $I \div V^{3/2}$ .

### 1.2 Focusing and Acceleration of the Beam

A first gap accelerates the ions to a few keV. It is followed by a two lenses system that defines the size of the beam at the plasma. A final gap accelerates the beam to the ground potential.

Because of the space charge effects in the region between the last lens and the plasma, the size of the beam is limited to a minimum of  $\sim 3$ mm in diameter for a 10  $\mu$ Amps beam. Higher current can be given out by the source, but this will enlarge the beam at the plasma.

The accelerating chamber is connected to the sweep chamber by a small aperture so as to provide differential pumping possibility.

### 1.3 The Deflection System

The deflection system is designed in order to reduce to a minimum the access to the plasma chamber. The first set of plates deflects the beam in a given direction. The second set acts in the opposite direction with a stronger field. The net effect is to focalize the beam (to the first order) at a given distance,  $f$ , from the second set of plates. The ion gun can then be connected to the plasma chamber through a small hole aperture. This will help maintaining a good vacuum in the gun chamber and will also simplify the determination of the initial conditions of the beam.

The sweep chamber should be as short as possible to reduce the space charge divergence of the beam.

## 2. The Detectors

The first element of a detector is the entrance slit that selects a particular secondary beam. This slit must be correctly positioned such as to look at the required plasma volume. The slit is oriented parallel to the main confining field (Fig. 1). The secondary ions enter the detector with different velocities and positions along the slit depending upon the deflection of the particles by the field.

The currents to be measured are of the order of the nAmps. One has then to worry about noises such as photoelectric effects due to the ultraviolets or soft X-rays generated by the plasma. To separate the signal from most of the sources of noise, one can use the energy of the ions which is much higher than everything produced by the plasma.

### 2.1 Energy Analyzer

The energy analyzer has the two functions of selecting the secondary ions over the plasma noise and of measuring their energy, which gives the electric potential.

A simple analyzer is shown in Fig. 7. The secondary ions selected by the slit are deflected by a uniform electric field. They follow a parabolic trajectory and are collected by two split plates.

The ions enter the detector with an energy equal to the initial accelerating voltage plus a small correction due to the potential at the secondary emission point. Ions with greater energy will travel farther and be collected mainly by one side of the split plates collector. The resulting unbalance in the collected current can then be amplified and fed back to the voltage applied to the detector such as to recenter the beam on the collector. The feed back signal is then function of the electric potential at the secondary emission points.

The ions enter the analyzer with different angles depending upon the position of the secondary emission points. Unfortunately, the feedback signal will also be dependent upon this angle. It is then important either to know the entrance angle or to find a geometry of fields that is not sensitive to the angle. This is approximately realized with the detector of Fig. 7 if the entrance angle is  $45^{\circ}$ . At this angle, the path length is maximum and is independent of the angle for small variations (see Fig. 9).

The performances of the energy analyzer can be further increased if one introduces a field free drift space as shown in Fig. 8. For any angles, between  $30^{\circ}$  and  $45^{\circ}$ , it is possible to optimize the geometry of the detector such as to minimize the dependence upon the angle (see Fig. 9). With this type of detector, resolutions of 1 Volt with a 10 KV ion beam have been obtained<sup>3</sup>.

Note that the total current of secondary ions can be measured simultaneously with the feedback voltage, i.e. the electric potential and the electronic density are measurable together.

## 2.2 Directional Analyzer

To measure the magnetic potential, one has to determine one component of the velocity of the secondary ions. Such a detector has been designed but not yet tested. Its principle is shown in Fig. 10.

The ions from a given secondary beam selected by the entrance slit enter the uniform field of a parallel plates condensator. The field is oriented in the direction of the component to be measured (let say the z-direction). After being deflected, the ions are collected by a set of double parallel plates. If the ions reach the collector with a non zero z-velocity, one set of the plates will collect most of the ions, whereas the other set will collect part of the secondary electrons emitted by the ions impact. A net

current will then circulate in the collector circuit of sign depending upon the sign of the z-velocity. This current can then be amplified and fed back to the deflecting voltage to keep the collector current to zero.

When the current is zero, the z-velocity at the entrance slit is given by

$$v_z^2 = \frac{W - \sqrt{W^2 - (q \cdot E \cdot \ell)^2}}{m} \quad (13)$$

where W is the energy of the secondary ions  
E the deflecting field  
q,m the charge and mass of the ions  
ℓ the length of the deflecting region

In most cases one will have  $W \gg qE\ell$ . The velocity will then be simply given by

$$v_z = \sqrt{\frac{qE\ell}{2m}} \quad (14)$$

With the proper shaping of the deflecting plates, this detector will be independent upon the other components of the velocity and on the position along the entrance slit of the secondary ions.

## VII OBJECTIVES, PLANNING AND COST EVALUATION

The long term objective of this development would be to install an IBP on TCA (or TCV). Before this, it is necessary to build a smaller system to see what are the problems related to the construction of an IBP and to study what can be measured with it.



Much work has already been done about the density and temperature measurements<sup>1,2,4</sup>. The electric potential has also been measured<sup>3,4</sup>, but one has to prove that it can be applied to a tokamak, the problem being the resolution of the detector.

The main objective in this project will be to show that the magnetic potential can be measured and to study the possibility of measuring density fluctuations.

The project will be divided in two parts. At first the ion gun and the detectors will be tested on a vacuum bench without plasma. In second, a linear arc discharge will be built and the IBP operated on it.

1. First Part of the Project :

Construction and Test of the Ion Gun and the Detectors

A low energy (10 KV) ion gun will be sufficient for this project. The construction of such a gun does not involve much difficulties. It has to be designed such as to provide good and controlable focusing of the beam. The spacial resolution of the diagnostic system depends much on this.

The power supply necessary to run the gun is divided in 3 parts :

1. a 10 KV, 100  $\mu$ Amps voltage supply to accelerate the beam.
2. a 2 KV, 1 mAmp for the extractor and the focusing of the beam.
3. a low voltage high current supply to heat the ion emitter.

The sweep plates will be driven by a saw tooth signal of maximum amplitude 5 KV and a minimum duration of 10 - 20 $\mu$ s. This requires a voltage supply of  $\pm 3$  KV, a high voltage differential amplifier and a variable saw tooth signal generator.

The detectors have not yet been fully designed. It is first necessary to study the behaviour of the ion collectors, particularly for the directional analyzer of Fig. 10.

The cost of the materials used for this project can be evaluated as :

(in frs. 1000.-)

Ion gun	1
Voltage supplies	5
Electronic material (sweeping amplifier, detector amplifiers, signal generator)	2
Vacuum system (Pyrex tubes, supports etc. It is not necessary to buy a new vacuum pump)	2
Total cost	<hr/> 10

This project requires about six months to be completed.

## 2. Second Part of the Project :

### Construction of a Hollow Cathode Arc Discharge and Study of the IBP Diagnostic System

To study the diagnostic method, one needs a plasma with the following characteristics :

Density	$10^{13} - 10^{15} \text{cm}^{-3}$
Ionization rate	$\geq 90\%$
Electronic temperature	$\geq 10 \text{ eV}$
Max. current density	$\sim 150 \text{ Amps/cm}$
Confining magnetic field	$1 \sim 2 \text{ KGauss}$
Duration of the discharge	$5 \cdot 10^{-3} \text{ s}$

These parameters should allow to test the measurement of the magnetic potential in conditions similar to a tokamak.

This type of plasma should be obtainable in a pulsed arc discharge. However, to have such a high ionization rate (>90%), it is necessary to differentially pump the plasma chamber and to use a gaz fed hollow cathode<sup>8</sup>. In this way, the density of neutrals is determined by the pressure in the vacuum chamber, whereas the plasma density is fixed by the pressure of gaz inside of the hollow cathode. The preionization can be obtained by a discharge inside of the cathode (between a coaxial electrode and the cathode cylinder) that will inject some plasma inside of the vacuum chamber as a plasma gun.

To be able to measure the magnetic potential, one needs to have a large enough azimuthal field  $B_\theta$ , i.e. a large enough current density  $j_z$ . The Kruskal limit imposes the following restriction on the size of the discharge :

$$\frac{B_\theta}{B_z} < \frac{2\pi r}{\ell} \quad (15)$$

where  $r$  is the radius and  $\ell$  the length of the plasma column. With  $B_\theta/B_z = 0.1$ ,  $\ell = 1\text{m}$ , the plasma radius must be larger than 1.6 cm.

To probe this plasma, we will need a Li or Na beam with energies between 2 - 10 KV.

The cost of this plasma device cannot be exactly evaluated yet as it is not fully designed. It depends mainly upon the vacuum pumps needed to maintain the differential pressure between the hollow cathode and the vacuum chamber. This in turn depends on the minimum pressure in the cathode needed to maintain the discharge.

A reasonable evaluation of the cost would be

	(in frs. 1000.-)
Vacuum pumps	40
Vessel (Pyrex tubes) and support structures	5
Coils for the magnetic field	2
Capacitor benches to feed the magnetic field coils and the plasma discharge	2
Tungsten cylinders for the cathode and anode	1
Control electronic	<u>10</u>
Total cost	60

To build this plasma arc discharge and to operate the IBP on it should take about one year of work.

The whole thesis work would then require a minimum of two years to be completed.

REFERENCES

- 1 Plasma Density Measurement by Ion Beam Probing  
F.C. Jobes, J.F. Marshall, R.L. Hickok  
Physical Review Letters, Vol. 22, No. 20, p. 1042 (1969)
- 2 Measurement of Plasma Electron Temperature with an Ion Beam Probe  
R.E. Reinovsky, W.C. Jennings, R.L. Hickok  
Phys.Fluids 16, No. 10, 1772 (1973)
- 3 A Direct Measurement of Plasma Space Potential  
F.C. Jobes, R.L. Hickok  
Nucl.Fusion 10, 195 (1970)
- 4 Spatially Resolved Instability Measurements with a Heavy Ion Beam  
Probe  
W.C. Jennings, R.L. Hickok, J.C. Glowienka  
7th Europ.Conf. on Contr.Fusion and Plasma Physics, Vol. 1, 183 (1975)  
see also references quoted in these articles
- 5 Magnetic Field Measurement in a High Temperature Plasma  
G. Tonetti, Master Thesis
- 6 Aluminosilicate Alkali Ion Sources  
R.E. Weber, L.F. Cordes  
Review of Scient. Instr. 37, 112 (1966)

- 7 Theory and Design of Electron Beams  
J.R. Pierce  
Van Nostrand, New York (1954)
  
- 8 Highly Ionized Hollow Cathode Discharge  
L.M. Lidsky, S.D. Rothleder, D.J. Rose, S. Yoshikawa  
Journal of Applied Physics 33, 8, 2490 (1962)

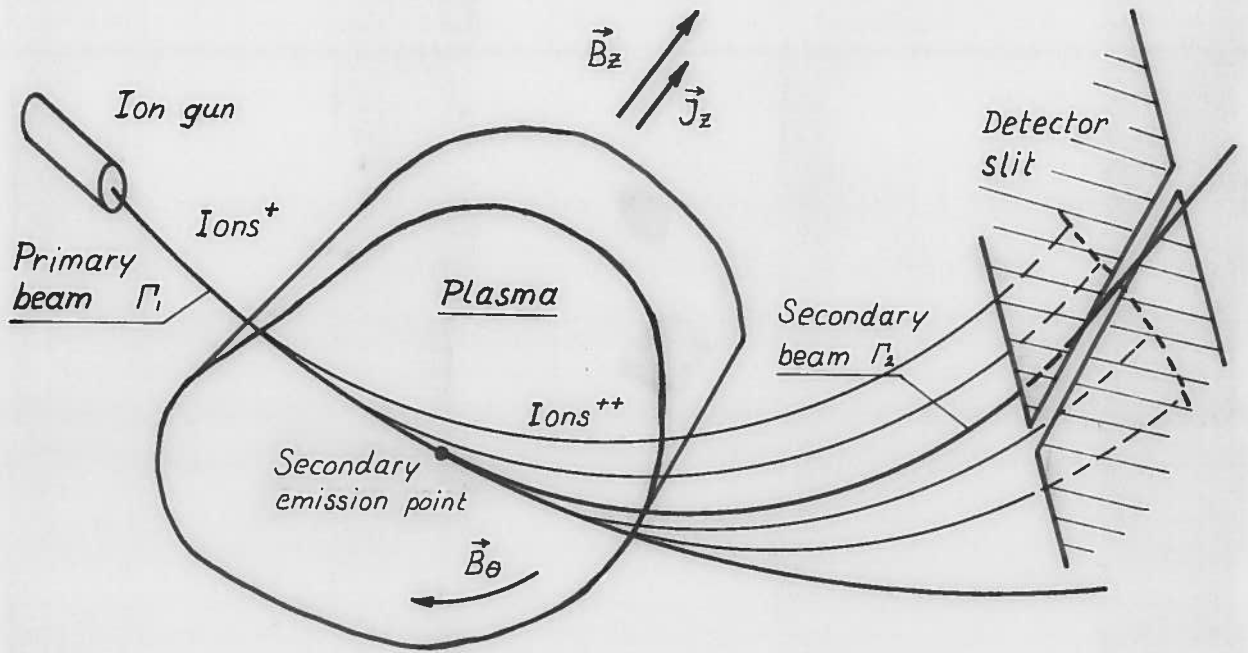


Fig. 1 Principle of the IBP

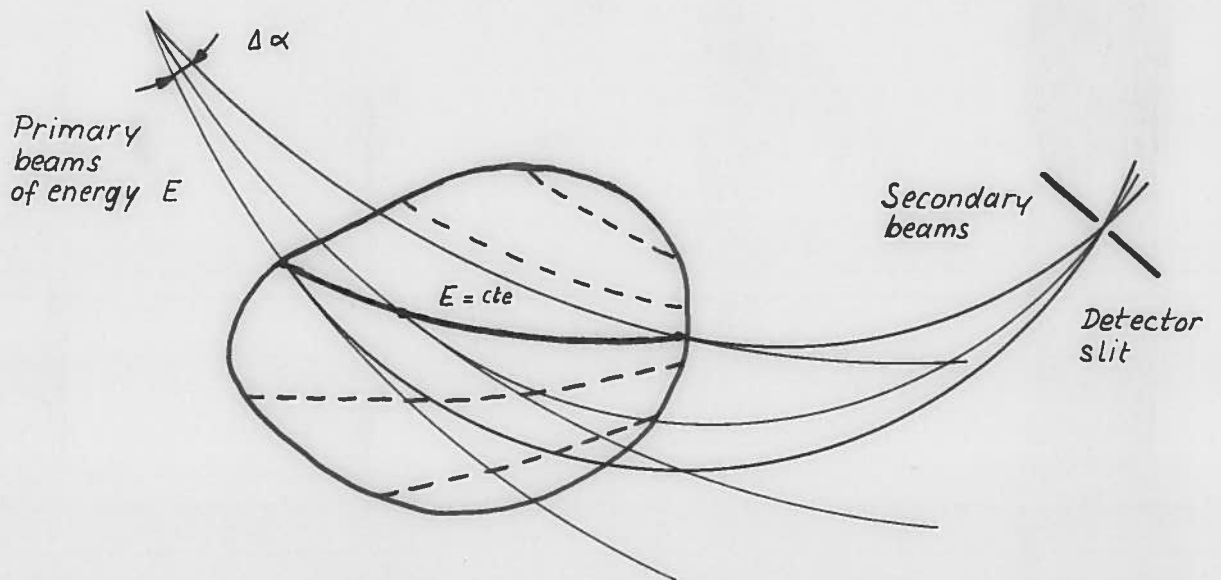


Fig. 2 By sweeping the beam, the detector samples the plasma along a line of constant energy. With another energy, the detector will look at another line  $E = cte$ .

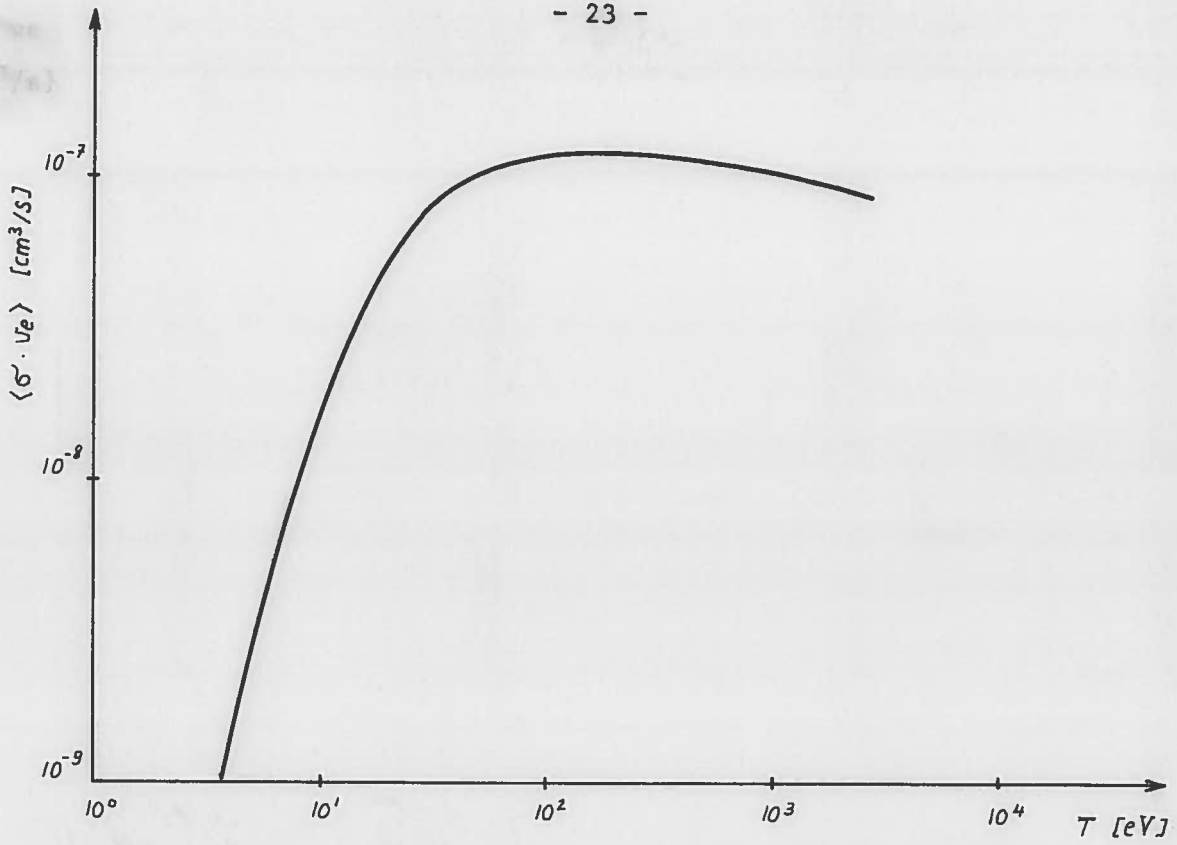
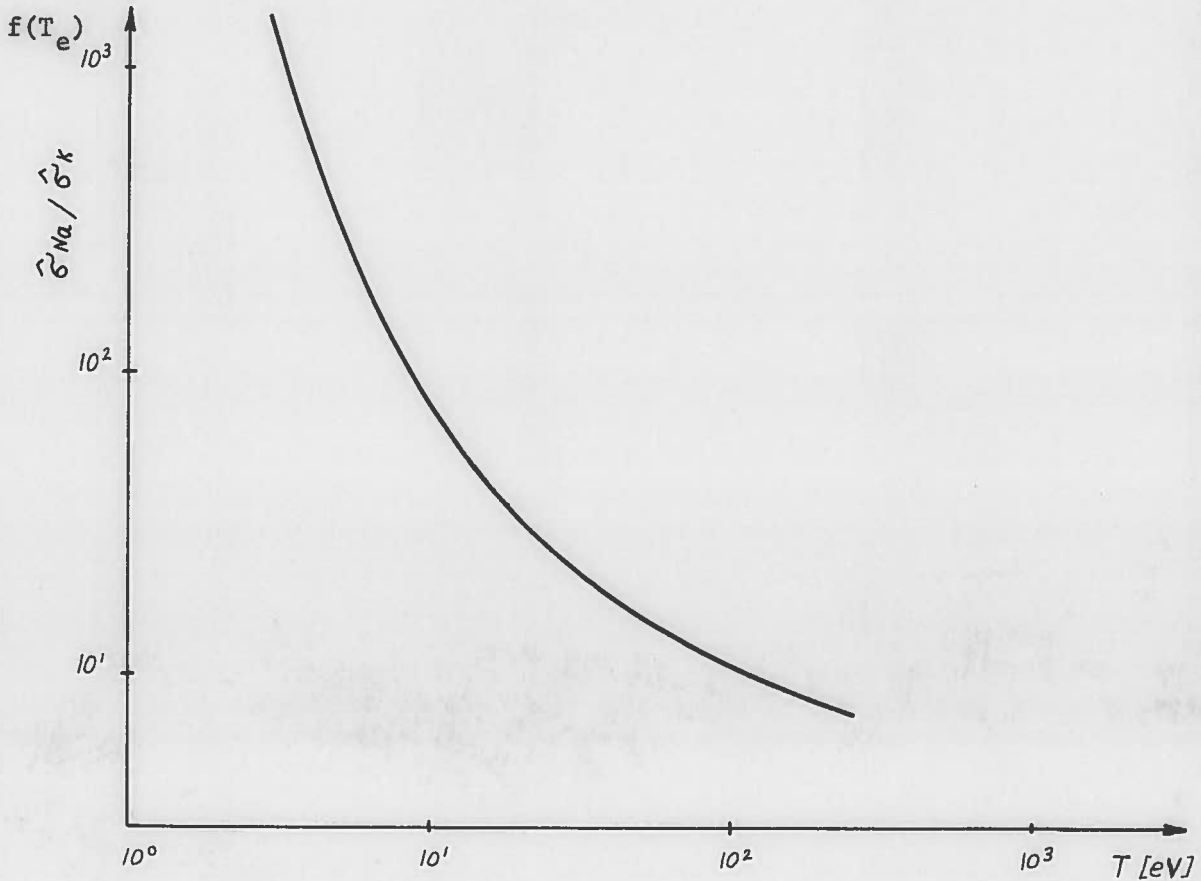


Fig. 3. Top Average cross section for  $\text{Tl}^+ + e^- \rightarrow \text{Tl}^{++} + 2e^-$   
Bottom Ratio of the effective cross sections  $f(T_e) = \frac{\hat{\sigma}_{\text{Na}}}{\hat{\sigma}_{\text{K}}}$   
for sodium and potassium ions.





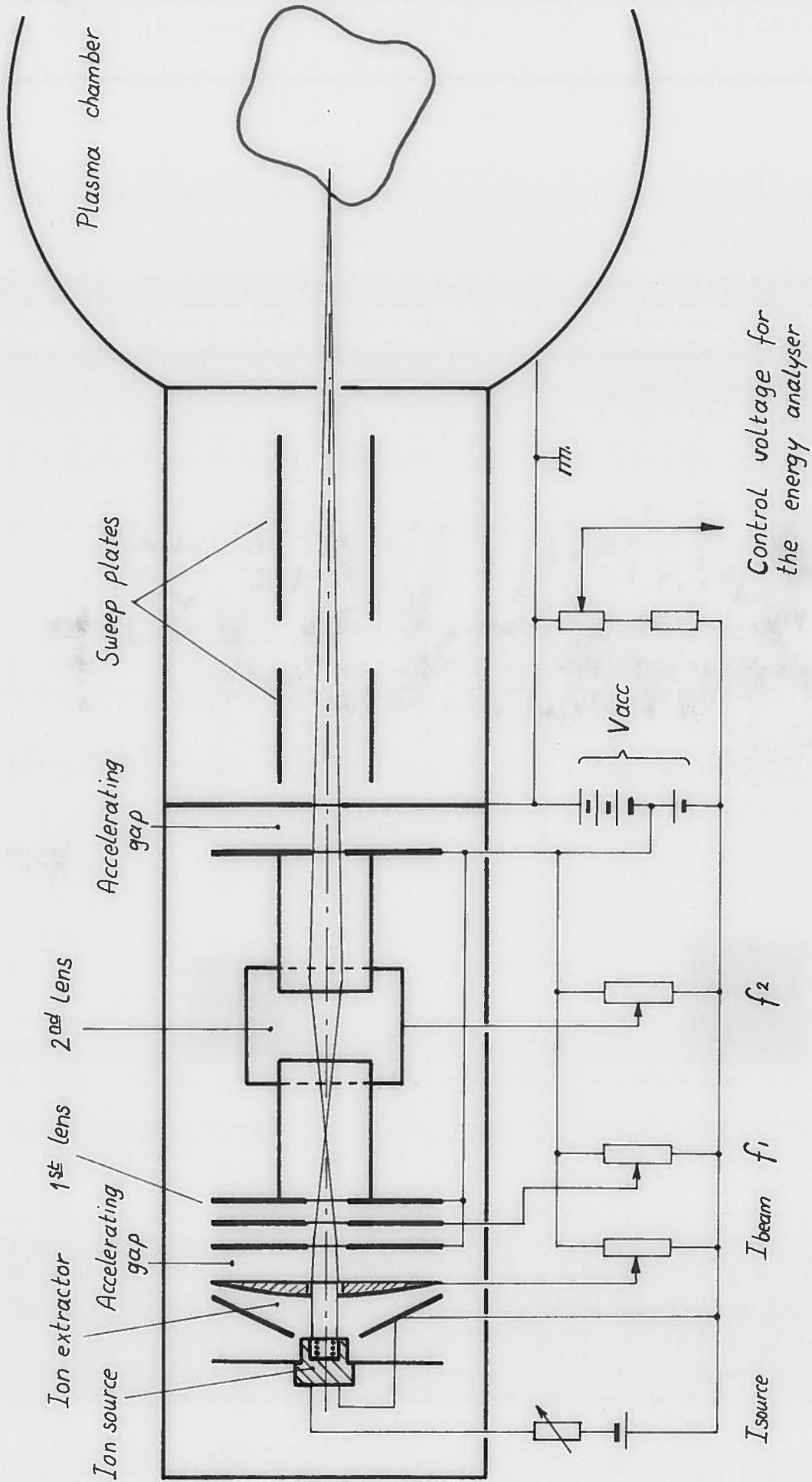


Fig. 4. Ion gun

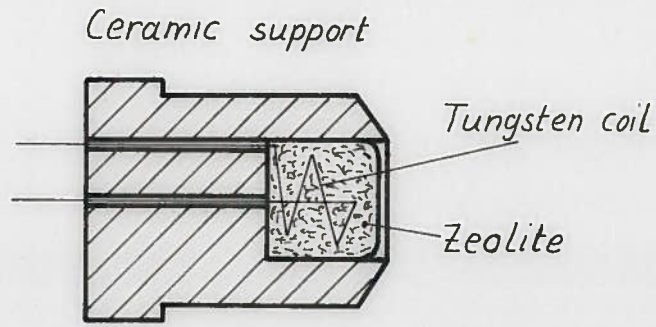


Fig. 5. Ion emitter

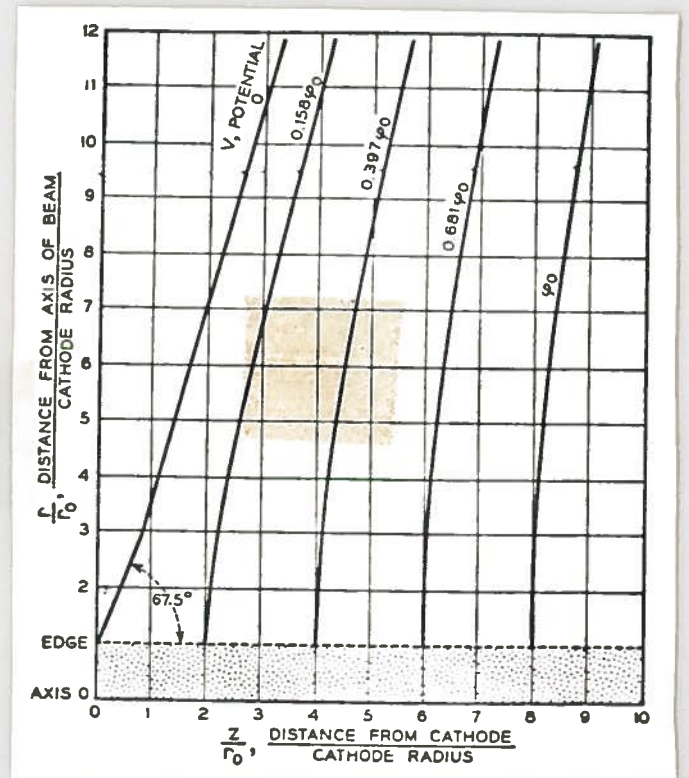
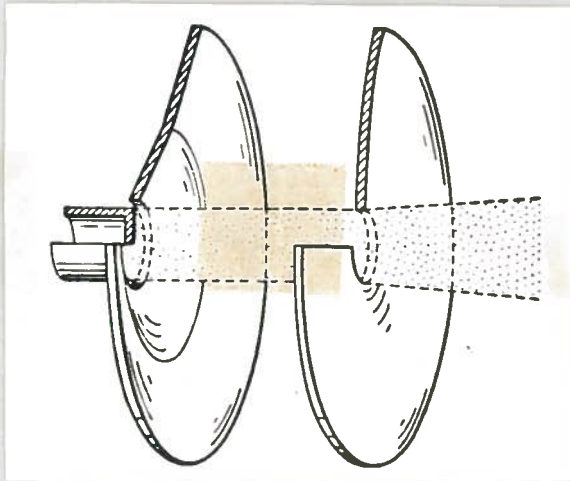
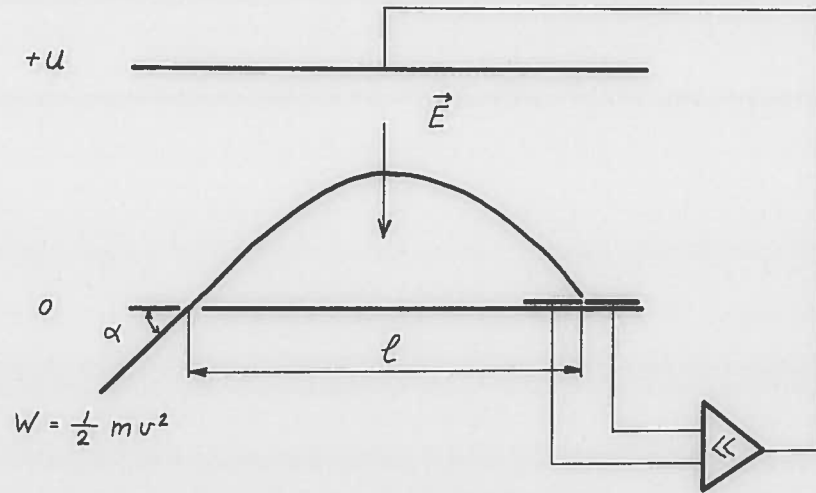
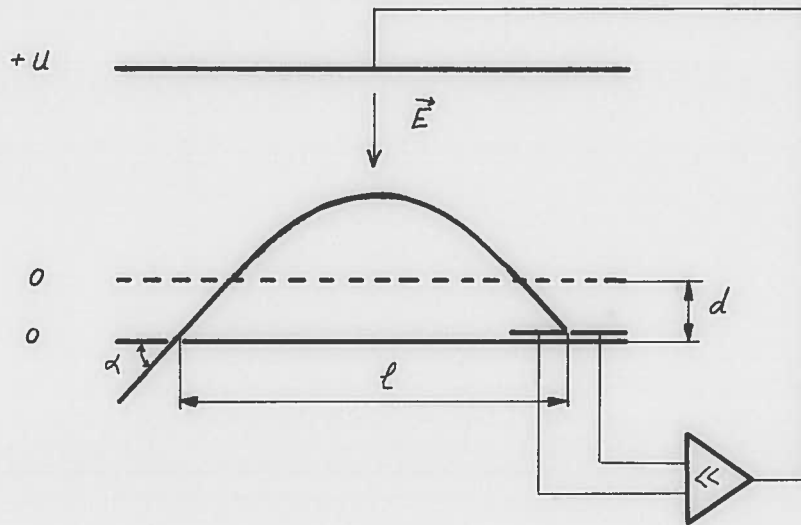


Fig. 6. Shape of the ion extractor electrodes (Pierce gun)



$$E = \frac{W}{q} \frac{2}{l} \sin 2\alpha = \frac{W}{q} \frac{2}{l} h(\alpha)$$

Fig. 7. Simple energy analyzer



$$E = \frac{W}{q} \frac{2}{l} \frac{\sin 2\alpha}{1 - \frac{2d}{l} \text{ctg} \alpha} = \frac{W}{q} \frac{2}{l} h(\alpha)$$

Fig. 8. Energy analyzer with second order focusing properties

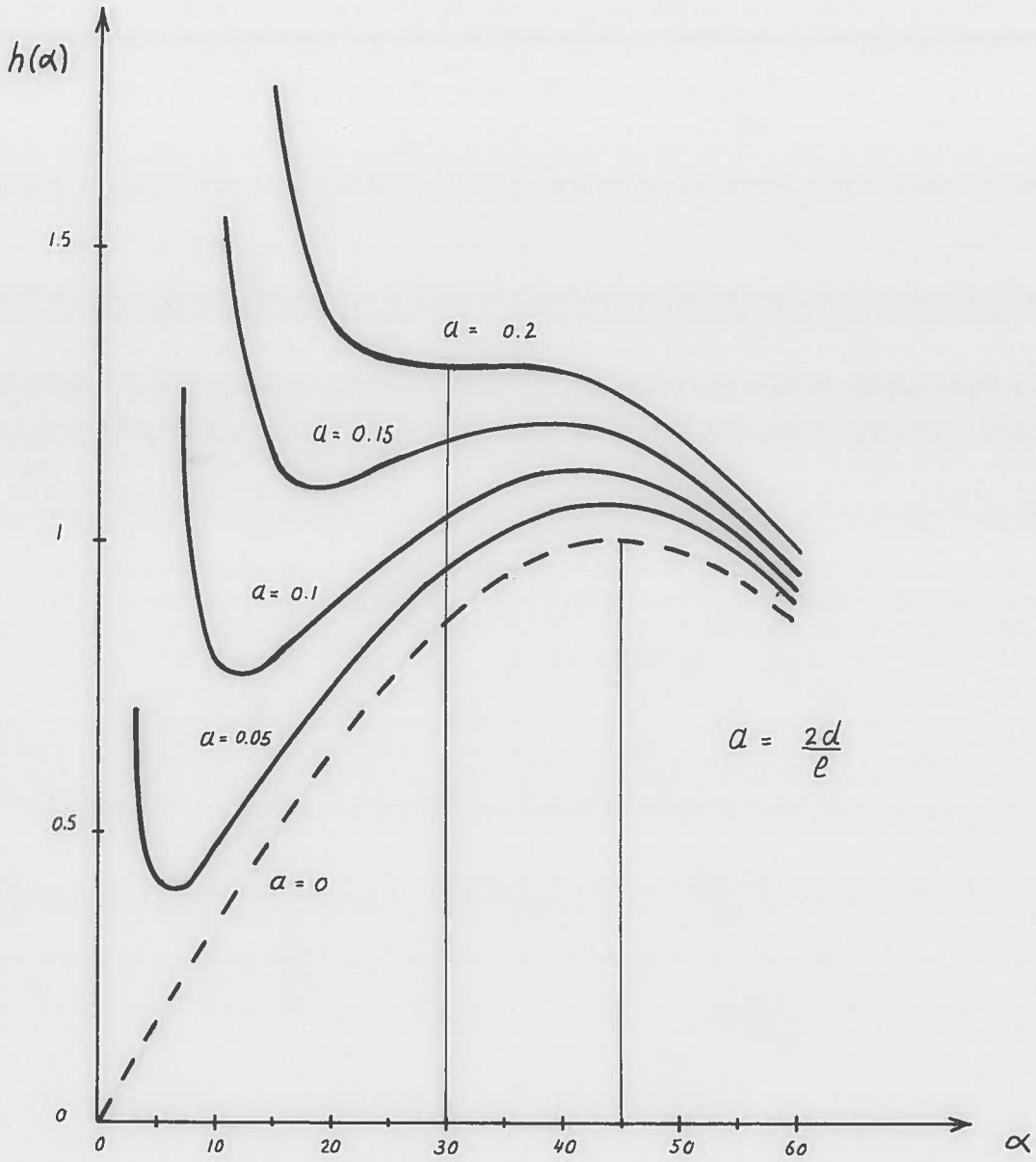


Fig. 9. Characteristic of the energy analyzers  
----- simple energy analyzer  
—— with second order focusing

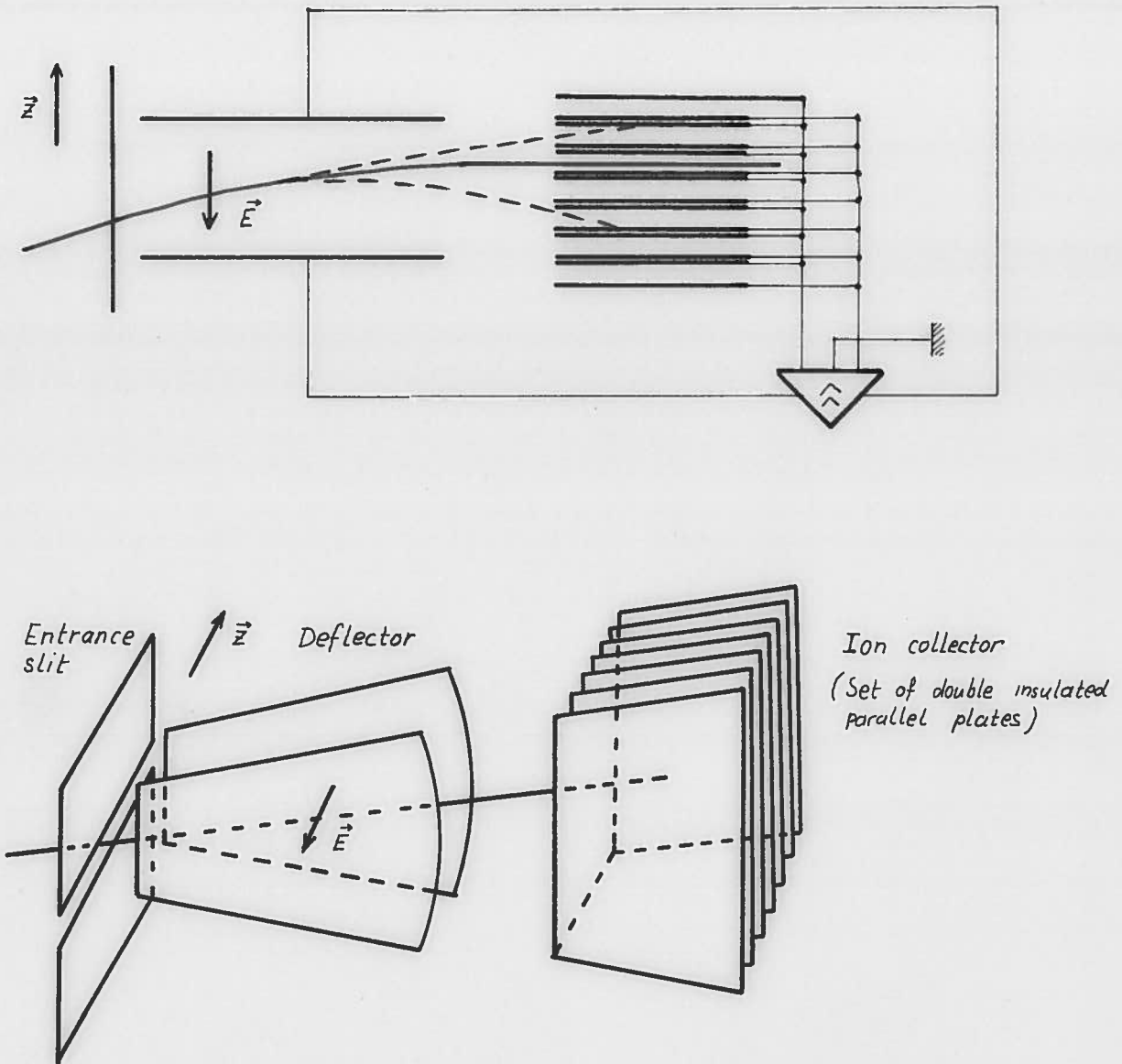


Fig. 10. Directional analyzer

This detector measures the component  $v_z$  of the velocity independently of the other components and of the position  $z$  along the entrance slit.